Research article

SLC7A5 is a lung adenocarcinoma-specific prognostic biomarker and participates in forming immunosuppressive tumor microenvironment

Yong Liu [a,1], Guoyuan Ma [b,1], Jichang Liu [a], Haotian Zheng [a], Gemu Huang [c], Qingtao Song [c], Zhaofei Pang [a,d,e,**], Jiajun Du [a,b,d,*]

[a] Institute of Oncology, Shandong Provincial Hospital, Shandong University, Jinan, 250021, Shandong, China
[b] Department of Thoracic Surgery, Shandong Provincial Hospital, Shandong University, Jinan, 250021, Shandong, China
[c] Amoy Diagnostics Co., LTD., Xiamen, 361010, Fujian, China
[d] Institute of Oncology, Shandong Provincial Hospital Affiliated to Shandong First Medical University, Jinan, 250021, Shandong, China
[e] Department of Oncology, Shandong Provincial Hospital Affiliated to Shandong First Medical University, Jinan, 250021, Shandong, China

ARTICLE INFO

ABSTRACT

Background: Amino acid metabolism participates in forming immunosuppressive tumor microenvironment. Amino acid transporters (AATs), as a gate for admission, remains to be studied.

Materials and methods: We identified LUAD-specific prognostic AATs, SLC7A5 by differential expression analysis, logistic regression, machine learning, Kaplan-Meier analysis, AUC value filtrating and Cox regression. Then differential expression and distribution of SLC7A5 were depicted. Copy number variation, DNA methylation, transcriptional factors and ceRNA network were investigated to explore potential mechanism causing differential expression. The prognostic and clinical relation were evaluated by Kaplan-Meier analysis, Cox regression analysis. GSEA and GSVA were used to analyze altered pathways between SLC7A5 high- and low-groups. The expression of HLA-related genes and immune checkpoint genes, and immune cells infiltration were detected. SLC7A5 expression in immune cells was evaluated by single-cell sequencing data. IPS and an independent immunotherapy cohort assessed response rates of patients with distinct SLC7A5 expression. Proliferation assay and wound healing assay validated the effects of SLC7A5 on proliferation and migration of LUAD cells. Western blotting and cell viability assays were performed to detect mTORC1 pathway activity and sensitivity to rapamycin.

Results: SLC7A5 was a LUAD-specific prognostic AAT and had significant differential expression in transcription and translation level. Methylation levels of cg00728300, cg00858400, cg12408911, cg08710629 were negative correlation with SLC7A5 expression. FOXP3 and TFAP2A were possible transcription factors and miR-30a-5p, miR-184, miR-195-5p may target SLC7A5 mRNA. SLC7A5 high-expression indicated poor prognosis and was an independent prognostic factor. mTORC1, cell cycle, DNA damage repair, response to reactive oxygen, angiogenesis, epithelial-mesenchymal transition (EMT) and various growth factors signaling pathways were activated in SLC7A5 high-expression group. Interestingly, SLC7A5 high-expression group had less immune-related genes expression and immune cells infiltration. Single-cell sequencing data also suggested SLC7A5 was down-regulated in various T cells, especially effector T cells. Moreover, high SLC7A5 expression indicated poor immunotherapy efficacy and higher sensitivity to inhibitors of mTORC1 pathway, cell cycle and angiogenesis. SLC7A5 deficiency abrogated proliferation, migration and mTORC1 pathway activity.

Conclusions: In summary, as a LUAD-specific prognostic AAT, SLC7A5 is involved in activation of multiple oncogenic pathways and indicates poor prognosis. Moreover, SLC7A5 may participate in forming immunosuppressive TME and is associated with low response of immunotherapy. SLC7A5 is promising to be a new diagnostic and prognostic biomarker and therapeutic target in LUAD.

* Corresponding author.
** Corresponding author.
E-mail addresses: pzfei1989@163.com (Z. Pang), dujiajun@sdu.edu.cn (J. Du).
[1] These authors contributed equally to this work.

1. Introduction

Lung cancer is one of the most common malignancies and remains the leading cause of cancer-related death worldwide [1]. Lung adenocarcinoma (LUAD), the most common histological subtype of lung cancer, accounts for approximately 40% of all lung cancer cases, raising a great threat to human health [2]. A comprehensive treatment consisting of surgery, radiotherapy, chemotherapy and targeted therapy is still the main treatment method [3]. Unfortunately, due to rapid progression, early metastasis and lack of accurate biomarkers, most patients have an unfavorable survival [4].

With the deepening understanding of the role of immunity on anti-tumors, immune checkpoint blockade (ICB) therapy (anti-PD-L1/PD-1/CTLA4 therapy) and chimeric antigen receptors (CAR) T cell therapy have emerged and revolutionized the treatment methods of cancer [5, 6]. Immunotherapy has considerably improved survival of LUAD patients. However, not all cancer patients can benefit from ICB therapy and only about one third of patients acquired stable alleviation [7]. Moreover, CAR T cell therapy in the solid tumor setting is also limited [8]. First, effector T cells must traffic to and penetrate into the tumor which involves extravasation, chemotaxis and stromal penetration [9]. Upon entering the tumor microenvironment (TME), the immune cell will encounter immunosuppressive conditions such as acid and hypoxia environment [10], numerous immune checkpoint ligands and immunosuppressive cells [8, 11, 12]. Chronic antigen engagement will result in T cell exhaustion and decrease the function of effector T cells [13]. Last, due to heterogeneity of tumor cells, some tumor cells will evade the CAR T cell detection [14]. As a result, it is urgently demanded to search for new biomarkers to identify cancer patients suitable for immunotherapy and feasible target to enhance anti-tumor immunity.

Due to rapid proliferation, Tumor cells have an extraordinarily elevated requirement for nutrients to sustain their demanding anabolic needs and energy production rates [15]. Thus, to satisfy the requirement, tumor cells rewire their metabolism activity including amino acid, glucose and fatty acid metabolism. Amino acids, as the basic unit of protein, is essential for both tumor cells and immune cells to survive and exert their function. Amino acid transporters (AATs) take responsible for the uptake of amino acids and have been reported to be upregulated in malignant tumor cell for acquiring more nutrients within TME [16]. At the same time, the reduction of nutrients and oxygen and release of immunosuppressive metabolites like lactate will generate a hostile environment for tumor-infiltrating lymphocytes (TILs), which makes it more difficult for TILs to compete with cancer cells for nutrients to support their anti-tumor functions [17]. It has been reported that the metabolic stress in TME can impair their response to tumor cells by altering the expression of AATs. For instance, XBP1 induction in CD4+ T cells inhibited the expression of the glutamine transporters SLC1A5, SNAT1, and SNAT2 under glucose deprivation, causing reduced glutamine uptake and oxidative phosphorylation, which limited IFN-γ production. In this feedback loop, decreasing expression of AATs would further impair the function of CD4+ T cells [18]. In addition, lack of glutamine and glucose in the TME may promote the development of regulatory T cells (Treg) rather than effector T cells such as T helper 1 and 17 cells. For example, overexpression of SLC1A5, SLC3A2 and SLC7A5 is obviously related to existence of Foxp3+ Tregs and indicates worse prognosis of breast cancer patients [17, 19, 20]. Although the reprogramming of amino acids metabolism brings us great challenge for anti-tumor therapy, it also implies us that rewiring amino acid metabolism by targeting tumor-specific AATs may break the bottleneck of anti-tumor therapy at present.

In this study, we identified LUAD-specific prognostic AATs, SLC7A5 by differential expression analysis, logistic regression analysis, machine learning, AUC value filtrating, Kaplan-Meier analysis and Cox regression. Then, we found SLC7A5 was significantly upregulated in the mRNA and protein levels of LUAD comparing to normal tissues and mainly distributed in plasma membrane, cytosol and vesicles. Moreover, we

investigated the potential mechanism leading to the aberrant expression by analyzing copy number variation (CNV), DNA methylation, transcriptional factors (TFs) and competing endogenous RNA (ceRNA) network. We demonstrated high SLC7A5 expression indicated worse prognosis and advanced pathological stage and was an independent prognostic factor. The results of functional enrichment analysis showed that SLC7A5 expression was tightly associated with mTORC1 pathway, cell cycle, DNA damage repair, response to reactive oxygen and immune. The landscape of TME reflected higher expression of HLA-related genes and immune checkpoints, immune cells infiltration and response to anti-tumor immunotherapy in SLC7A5 low-expression group. Interestingly, SLC7A5 was commonly low expression in immune cells within TME. Patients with high SLC7A5 expression were more sensitive to chemotherapy drugs targeted mTORC1 pathway, cell cycle and angiogenesis and possessed higher scores of amino acids, EMT, DNA damage, hypoxia and tumor stemness but not tumor mutation burden (TMB). In vitro, SLC7A5 deficiency impaired the ability to proliferate, migrate and mTORC1 pathway activity. Consequently, it is promising that SLC7A5 is used to stratify the patients for immunotherapy and chemotherapy and predict the prognosis of LUAD patients. Upregulating SLC7A5 expression in TILs and downregulating it in tumor cells may strengthen TILs to compete for nutrients and reshape immunosuppressive TME.

2. Materials and methods

2.1. LUAD dataset acquisition and preprocessing

The transcriptomic profiles and corresponding clinical information were retrieved from The Cancer Genome Atlas (TCGA, http://cancergenome.nih.gov/) and Gene Expression Omnibus (GEO) databases (https://www.ncbi.nlm.nih.gov/). The clinical information data was showed in Table 1. The multiple GEO cohorts (GSE3141, GSE13213, GSE31210, GSE30219, GSE37745, GSE50081) were integrated and Batch effects were removed by the combat algorithm in the "sva" package. The TCGA LUAD cohort included 535 tumor samples and 59 normal samples as the training cohort and the integrated GEO cohort included 719 tumor samples as the validation cohort. CNV and DNA methylation

Table 1. The clinical information data of LAUD patients from TCGA and GEO databases.

Variables	Discovery Cohort	Validation Cohort
	TCGA (504)	GEO (719)
Gender		
Male	234 (46.40%)	342 (47.60%)
Female	270 (53.60%)	319 (44.40%)
NA	-	58 (8.10%)
Age at Diagnosis		
Mean (SD)	65.30 (10.03)	62.22 (9.43)
Stage		
I	270 (53.60%)	480 (66.80%)
II	119 (23.60%)	128 (17.80%)
III/IV	107 (21.30%)	43 (6.00%)
NA	8 (1.60%)	68 (9.50%)
Survival Event		
Alive	321 (63.70%)	433 (60.20%)
Dead	183 (36.30%)	286 (39.80%)
Median Survival Time		
OS, Days (IQR)	652.5 (710.50)	1470 (1595.05)
PFS, Days (IQR)	523 (608.75)	-
Treatment Type		
Chemotherapy	259 (51.40%)	-
Radiotherapy	245 (48.60%)	-

SD: standard deviation; IQR: inter-quartile range.

data were downloaded from UCSC Xena (https://tcga.xenahubs.net) [21]. Using Clinical Proteomic Tumor Analysis Consortium database (CPTAC, http://proteomics.cancer.gov/), the proteomic profiles of LUAD were obtained and normalized by 'impute'. An immunotherapeutic cohort with ipilimumab was used to validate the immunotherapeutic response [22]. In addition, 51 LUAD and 8 adjacent normal tissues were collected from the Department of Thoracic Surgery, Shandong Provincial Hospital. The prognostic information was also followed up.

The ethics committee approval was granted by the Ethics Committee of Shandong Province Hospital (approval number: SWYX: NO. 2022-263). The requirement for written informed consent was waived. All procedures involving human participants were performed in accordance with the 1975 Helsinki declaration and its later amendments.

2.2. Identification of LUAD-specific prognostic AATs

The genes coding AATs were collected from the published literature [23]. For acquiring LUAD-specific AATs, differentially expressed genes coding AATs between LUAD and normal tissue were screened out by "limma" package ($P < 0.05$, |Log_2fold change| > 0). The logistic regression analysis ($P < 0.05$), Support Vector Machine (SVM) and Random Forest (RF) were used to further identify LUAD-specific AATs. The residual and area under curves (AUC) were applied to evaluate the efficacy of SVM and RF. To assess prognostic AATs, the Kaplan Meier analysis ($P < 0.001$), AUC value filtering (AUC >0.7), univariate and multivariate Cox regression ($P < 0.05$) were performed. Finally, the LUAD-specific and prognostic AATs were identified by intersecting the two parts.

2.3. Differential expression and distribution of SLC7A5 between LUAD and normal tissue

The differential expression of SLC7A5 in the transcription and translation levels was analyzed by TCGA and CPTAC data. Moreover, the difference between tumor and adjacent normal tissue was also detected. Eight pairs of LUAD and adjacent normal tissues from Shandong Province Hospital were detected for SLC7A5 mRNA expression by quantitative real-time polymerase chain reaction (qRT-PCR). The SLC7A5 mRNA and protein expression in LUAD cell lines including A549, PC9, HCC827, H1975 cells were compared by qRT-PCR and Western blot. The Human Protein Atlas (HPA, https://www.proteinatlas.org/) provided the immunohistochemistry staining image of SLC7A5 in LUAD. Using TIMER, the pan-cancer differential expression profiles of SLC7A5 were obtained. The SLC7A5 mRNA expression in normal human tissues and organs from GTEx, Illumina, BioGPS, and SAGE was displayed. The distribution pattern in cell was depicted in the GeneCards (https://www.genecards.org/). By immunofluorescence staining, the distribution of SLC7A5 in HCC827 and A549 cell was displayed.

2.4. CNV analysis of SLC7A5

Using the CNV data of LUAD, the difference of CNV of SLC7A5 between LUAD and normal samples was investigated. The correlation of SLC7A5 expression and CNV was also analyzed.

2.5. DNA methylation analysis of SLC7A5

Based on the DNA methylation data of LAUD, we analyzed the methylation levels of various sites of SLC7A5 and their association with prognosis. Further, we identified the prognostic methylation sites whose methylation levels were negatively related to SLC7A5 expression.

2.6. Identification of transcription factors

The promotor sequences of SLC7A5 were obtained by the National Center for Biotechnology Information (NCBI, https://www.ncbi.nlm.nih.gov/). 2000 bp upstream and 100 bp downstream of initiation site were considered as promotor sequences. The PROMO website (http://alggen.lsi.upc.es/cgi-bin/promo_v3/promo/promoinit.cgi?dirDB=TF_8.3) was utilized to predict the TFs. The fault tolerance was set to zero. The predicting TFs were intersected with the upregulated genes in LUAD.

2.7. Construction of the competing endogenous RNA (ceRNA) network

Based on starBase database (https://starbase.sysu.edu.cn/), the miRNAs targeted SLC7A5 were predicted [24]. When the miRNAs met the following conditions, the miRNAs were allowed for further analysis. (1) the correlation coefficient of miRNA and SLC7A5 < -0.2, $P < 0.05$; (2) Log_2fold change < -1, $P < 0.05$; (3) patients with the high miRNA profiles had higher overall survival (OS), $P < 0.05$. Then we predicted the lncRNAs targeted the miRNAs by starBase again. The lncRNAs meeting the following conditions were screened out. (1) the correlation coefficient of lncRNA and SLC7A5 > 0, $P < 0.05$; (2) the correlation coefficient of lncRNA and qualified miRNA < -0.1, $P < 0.05$; (3) Log_2fold change >0, $P < 0.05$. The ceRNA network was drawn by Cytoscape (version 3.9.1).

2.8. Analysis of prognosis and the clinicopathological correlation

The correlation of SLC7A5 expression and clinicopathological features was analyzed including age, gender, pathological stage, race, tumor site and treatment type. The Xtile software was used to determine the optimal cutoff value. According to the cutoff value, the LUAD patients were divided into SLC7A5 high- and low-expression groups. The OS and progression-free survival (PFS) curves were plotted based on TCGA LUAD data and Kaplan-Meier Plotter website (https://kmplot.com/analysis/). The data from GEO and Shandong Province Hospital were used for external validation of OS. In addition, univariate and multivariate Cox regression were performed to evaluate the independent prognostic factors from SLC7A5 expression and clinical features.

2.9. Functional enrichment analysis

TCGA LUAD samples were sorted by SLC7A5 expression. The top 100 samples with high expression and the end 100 samples with low expression were extracted. GO enrichment and KEGG pathway analyses were used to explore the potential biological processes (BP), cellular components (CC), and molecular functions (MF) of different expression genes between SLC7A5 high- and low-expression groups. FDR q value <0.05 was considered statistically significant. The significant GO pathways were displayed in the form of bubble plots by https://www.bioinformatics.com.cn, a free online platform for data analysis and visualization. Using the hallmark gene sets as the reference gene set and setting the adjusted P value to <0.05 and the |Log_2fold change| >0.1 as the cutoff criteria, GSVA was performed between SLC7A5 high- and low-expression group by GSVA package in R.

2.10. Exploration of tumor microenvironment landscape

The "estimate" package in R was applied to evaluate the immune score, stromal score, estimate score and tumor purity of each sample in the SLC7A5 high- and low-expression groups. The differences of 24 HLA-related molecules between SLC7A5 high- and low-expression groups were analyzed. The correlation of SLC7A5 and immune checkpoints was investigated. Tumor Immune Dysfunction and Exclusion (TIDE) algorithm was applied to distinct tumor immune evasion mechanisms, including dysfunction of tumor infiltrating cytotoxic T lymphocytes (CTLs) and exclusion of CTLs by immunosuppressive factors [7]. We calculated and compared the T cell dysfunction and exclusion scores between SLC7A5 high- and low-expression groups, respectively. To explore immune cells infiltration, the correlation of SLC7A5 expression and various immune cells including activated myeloid dendritic cell, CD4^{+} memory and effector T cell, M1 and M2 macrophage, B cell, monocyte et al. was investigated by multiple platforms such as XCELL,

TIMER, QUANTISEQ, MCPCOUNTER, EPIC, CIBERSORT-ABS, CIBER-SORT. Using the interactive web server (http://lung.cancerpku.cn), SLC7A5 expression was shown in multiple T cell subtypes, which was based on the single-cell sequencing of non-small cell lung cancer [25].

2.11. Analysis of immunotherapy efficacy and the sensitivity of chemotherapy drugs

Immunophenoscore (IPS) is a superior predictor of response to anti-CTLA-4 and anti-PD-1 regimens. The scoring system integrates the determinants of tumor immunogenicity and characterize the cancer antigenomes and intratumoral immune landscapes [26]. The distinction of IPS between SLC7A5 high- and low-expression groups was explored. An independent metastatic melanoma-related immunotherapy cohort receiving ipilimumab (anti-CTLA4 monoclonal antibody) was used for an external validation. The prognosis and response rates of SLC7A5 high- and low-expression groups in this cohort were assessed. The R package "pRRophetic" was applied to quantify the half maximal inhibitory concentration (IC50) of chemotherapy drugs [27].

2.12. Analysis of correlation between SLC7A5 expression and other malignant indicators

42 differential expressed genes encoding amino acid transporters was collected and SARRIO_EPITHELIAL_MESENCHYMAL_TRANSITION_UP. v7.5.1.gmt, WP_DNA_DAMAGE_RESPONSE.v7.5.1.gmt, HALLMAR-K_HYPOXIA.v7.5.1.gmt were downloaded from GSEA website as input files. By single sample GSEA (ssGSEA), we calculated amino acid score (AA score), EMT, DNA damage response and hypoxia scores of each LUAD patient. Cancer stemness scores were acquired from TCGA including DNAss and RNAss. In addition, the correlation of SLC7A5 and the other AATs expression was further analyzed. TMB of patients from TCGA patients was calculated. Then, the correlation between SLC7A5 expression and these malignant indicators was assessed by Pearson correlation. The landscape of gene mutations in SLC7A5 high- and low-expression groups was depicted.

2.13. qRT-PCR

Total RNA was extracted from LUAD frozen tumor tissues, the corresponding peritumoral normal tissues and cells using RNAiso Plus (Takara, Dalian, China). The mRNA (500ng) was converted into cDNA using PrimeScriptTM RT reagent Kit with gDNA Eraser (Takara, Japan). Then, cDNA was amplified with SYBR Premix Ex Taq (TliRNaseH Plus, Takara, Japan). The conditions for the PCR reactions were 10 min at 95 °C followed by 40 cycles of 15 s at 95 °C and 1 min at 60 °C. mRNA levels were assayed by qRT-PCR using the Roche LightCycler® 480 system. $2^{-\Delta\Delta Ct}$ method was used to obtain relative quantitation (RQ) values, with 18S rRNA as endogenous control. The list of primers was shown in supplementary table 1.

2.14. Cell culture and transfections

All cell lines were purchased from the Procell, Wuhan, China. A549 cells were cultured in F12K (HyClone, USA), and the other cell lines were cultured in RPMI H1640 (HyClone, USA), supplemented with 10% fetal bovine serum (BI, Israel) in a humidified atmosphere of 5% CO_2 and 37 °C according to protocol. SLC7A5 siRNAs (Transheepbio, Shanghai, China) were transfected into cells using jetPRIME (Polyplus-transfection, Illkirch, France) for transient transfection according to the manual.

2.15. Proliferation assays

Cells were resuspended and seeded in 96-well plate with a density of 3000 cells per well. After 6 hours, the first plate was fixed with 10% cold trichloroacetic acid for at least 24 h. Then the other samples were

collected in this way every 12 h. After all the samples were fixed, the plates were washed five times by submersion in tap water and excess water was removed. Then Sulforhodamine B sodium salt (SRB) (Sigma, USA) was added and stained them for 30 min. Next the plates were washed three times by 1% (vol/vol) acetic acid. After the plates were dry, 150 μl 10 mmol/L Tris was added to each well. Finally, the absorbance was measured at 562 nm in a microplate reader (Thermo Fisher, USA).

2.16. Cell viability assay

Cell viability was determined using Sulforhodamine B sodium salt dyeing method. Briefly, cells were resuspended and seeded in 96-well plate with a density of 7000 cells per well. After 6 hours, the cells adhered to the wall and indicated compound was added with a certain concentration gradient. Then, culturing for 48 hours, the plates was fixed with 10% cold trichloroacetic acid for at least 24 h and washed five times by submersion in tap water and excess water was removed. Then Sulforhodamine B sodium salt (SRB) (Sigma, USA) was added and stained them for 30 min. Next the plates were washed three times by 1% (vol/vol) acetic acid. After the plates were dry, 150 μl 10 mmol/L Tris was added to each well. Finally, the absorbance was measured at 562 nm in a microplate reader (Thermo Fisher, USA). The results were analyzed by Graphpad Prism 8.

2.17. Western blot analysis

Protein samples were dissolved in RIPA buffer complemented with Phenylmethanesulfonyl fluoride (Beyotime Biotechnology, Shanghai, China). The concentrations of extracted proteins were measured using BCA kit (Beyotime Biotechnology, Shanghai, China). Equivalent amounts of total protein extract were separated on 10% SDS-PAGE gels (90 V for 30 min and 120 V for 60 min) and transferred to polyvinylidene fluoride membranes (100 V, 100min). Then membranes were blocked for 1 h at room temperature in 5% BSA solution and incubated with appropriate primary antibody overnight at 4 °C. The primary antibodies were listed as followed: SLC7A5 (LAT1) (Cell Signaling Technology, USA: 1:1000); GAPDH (Santa Cruz, USA: 1:1000); AKT (Invitrogen, USA: 1:1000); p-ATK (Ser473) (Cell Signaling Technology, USA: 1:1000); mTOR (Proteintech Group, USA: 1:1000); p-mTOR (Ser2448) (Santa Cruz, USA: 1:1000). After washing with TBST, the membrane was incubated with corresponding HRP-labeled secondary antibody (Santa Cruz, USA: 1:10000) for 1 h. The bands were visualized using ECL kit and FluorChem E system (Proteinsimple, USA).

2.18. Wound healing assay

Cells were plated in a 12-well plate until 95% confluence and monolayers were scratched with a 200 μl pipette tip. Then the cells were maintained in corresponding culture medium supplemented with 2% fetal bovine serum at 37 °C under 5% CO_2. Cell migration was recorded at 0 h, 12 h, 24h, 36h after wound scratch. Three independent experiments were performed. The area of wound healing were measured by Image J.

2.19. Immunofluorescence

HCC827 and A549 cells were grown on glass coverslips in 24-well plates until about 90% density. Cells were fixed with ice-cold 4% Paraformaldehyde for 20 min and permeabilized with 0.2% Triton X-100 for 10 min. Cells were then washed with PBS, blocked in 10% goat serum albumin for 30 min and incubated with anti-SLC7A5 (Cell Signaling Technology, USA: 1:200) in 10% bovine serum albumin at 4 °C overnight. Subsequently, cells were rinsed with PBS and incubated with Alexa Fluor 594 (goat anti-rabbit) for SLC7A5 detection for 1 h at room temperature in the dark. Specimens were then washed with PBS, counterstained with Hoechst (Beyotime Biotechnology, Shanghai, China),

mounted and examined using a fluorescence microscope (Olympus, Milan, Italy).

2.20. Statistical analysis

The statistical analyses in this study were generated by R (version 4.1.3), Graphpad Prism 8. SPSS (version 26.0) was used for logistic regression analysis. When data were quantitative, statistical significance for normally distributed variables was estimated by Student's t-tests, and nonnormally distributed variables were analyzed by the Wilcoxon rank-sum test. When comparing more than two groups, Kruskal-Wallis tests and one-way analysis of variance were used as nonparametric and parametric methods, respectively. Kaplan-Meier survival analysis was tested by log-rank test. The correlation was tested by Spearman Correlation test. Two-sided $P < 0.05$ was considered statistically significant unless otherwise stipulated.

3. Results

3.1. Identification of LUAD-specific and prognostic AATs

The process identifying LUAD-specific and prognostic AATs was shown in Figure 1. From the published literature, a total of 61 AATs were admitted into differential analysis. 42 differential expressed AATs were identified (Supplementary Figure 1A). By logistic regression analysis, 38 AATs were qualified (Supplementary table 2). Comparing the residual and AUC, RF possessed higher efficacy than SVM in identification of LUAD-specific AATs (Supplementary Figure 1B-1D). According to the minimal error of cross-validation, we determined the number of trees. The variable importance of the output results (Gini coefficient method) was assessed from the perspective of decreasing mean square error and decreasing accuracy. Then 12 genes with an importance >2 were selected as candidate genes by RF (Supplementary Figure 1E-1F). Then 12 genes with scores of importance >2 were selected by RF (Supplementary Figure 1E-1F). Intersecting the above results, 12 AATs were considered as LUAD-specific, which were SLC7A7, SLC25A13, SLC1A1, SLC15A3, SLC38A7, SLC1A4, SLC7A5, SLC25A22, SLC7A11, SLC7A10, SLC25A12 and SLC43A2. To get prognostic AATs, the Kaplan Meier

analysis ($P < 0.001$), AUC value filtering (AUC >0.7), univariate and multivariate Cox regression ($P < 0.05$) were performed and there were 26, 11, 13 and 6 AATs, respectively (Supplementary Figure 1G, 1H). The common AAT between LUAD-specific and prognostic AAT was SLC7A5/LAT1 (Supplementary Figure 1I).

3.2. Differential expression and distribution of SLC7A5 between LUAD and normal tissue

The mRNA and protein levels of SLC7A5 all displayed significantly differential expression between LUAD and random or paired normal tissues from TCGA and CPTAC databases ($P < 0.001$) (Figures 2A-2D). 8 paired LUAD and paracancerous tissues from Shandong Province Hospital also showed SLC7A5 was tend to be upregulated in LUAD (Figure 2E). In LUAD cell lines, A549 cell had the most predominant SLC7A5 mRNA expression than other three. HCC827 was the second and PC9, H1975 both had low expression of SLC7A5 (Figure 2F). The transcription and translation levels of SLC7A5 were basically consistent in the four LUAD cell lines (Figure 2G). The immunohistochemistry staining image from HPA suggested SLC7A5 was easily detected in LUAD (Supplementary Figure 2A). The SLC7A5 mRNA expression was displayed in multiple normal human tissues and organs by GTEx, Illumina, BioGPS, and SAGE (Supplementary Figure 2B). By TIMER, SLC7A5 expression was upregulated in multiple tumors such as bladder cancer, esophageal cancer and Uterine Corpus Endometrial Carcinoma et al (Figure 1H). To explore the distribution of SLC7A5 in cells, we downloaded the pattern diagram from the GeneCards, which demonstrated that SLC7A5 was mainly located in plasma membrane, cytosol, vesicles (Supplementary Figure 2C). By immunofluorescence staining, it was found that SCL7A5 was diffusely distributed in cell membrane and cytosol of HCC827 and A549 cells. Almost no SLC7A5 entered cell nucleus (Figure 1I).

3.3. The potential mechanisms of differential expression of SLC7A5

Aiming to reveal the reasons for differential expression of SLC7A5 in LUAD, we explored three aspects including CNV, DNA methylation level, TFs and ceRNA regulatory network. Totally, 555 LUAD samples were
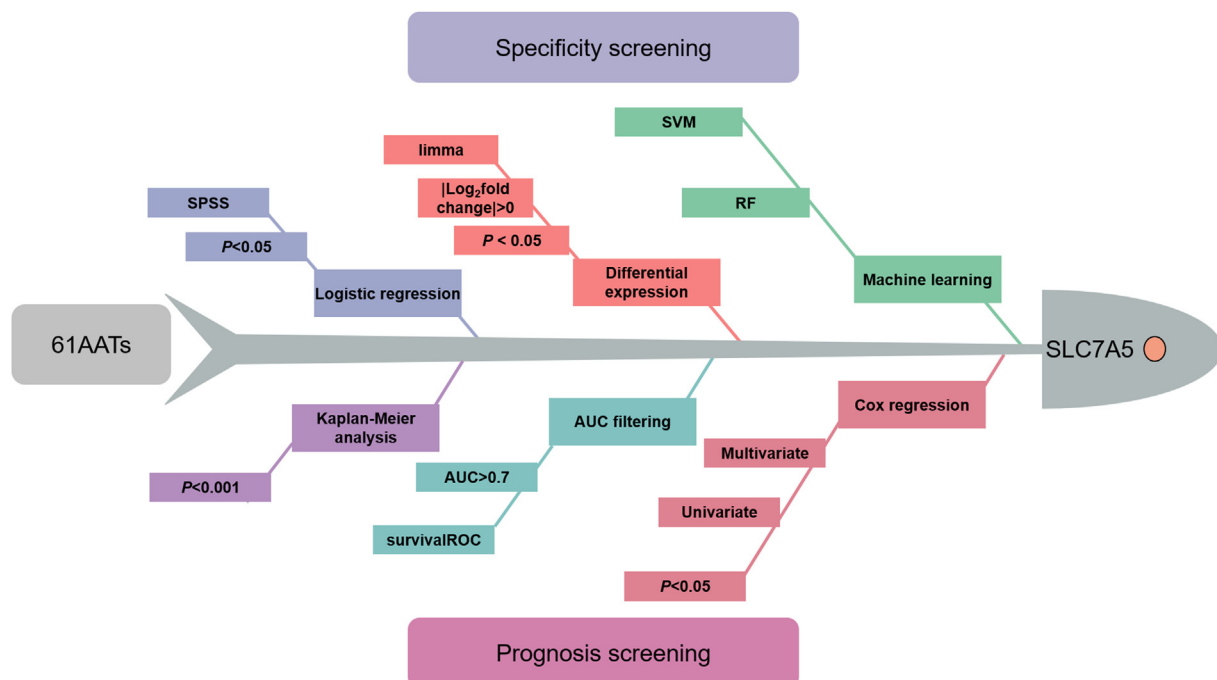

Figure 1. The flow chart of identifying LUAD-specific prognostic amino acid transporters (AATs).
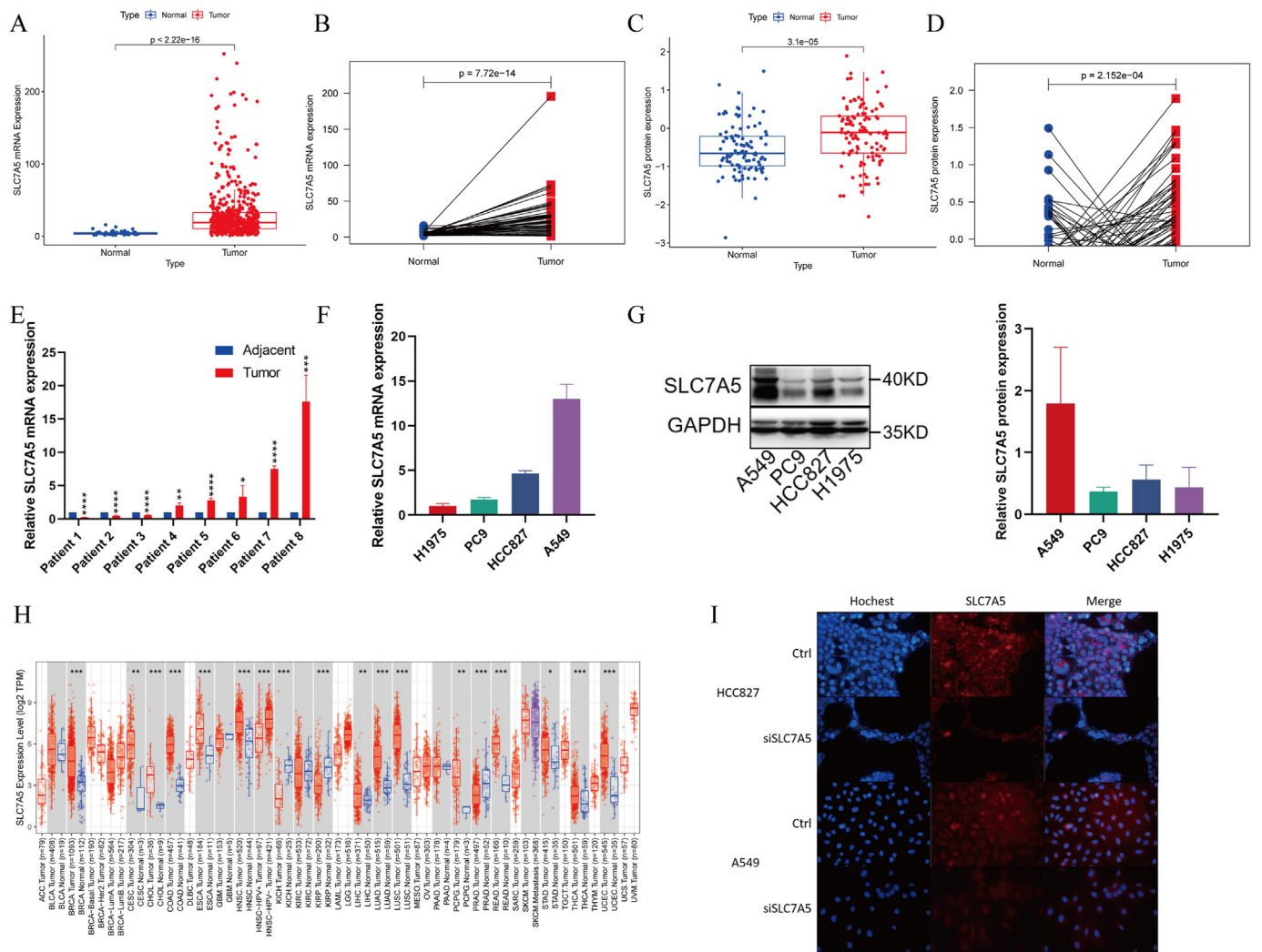
Figure 2. The differential expression and distribution of SLC7A5 in LUAD. (A) mRNA expression of SLC7A5 in TCGA LUAD vs normal tissues. (B) mRNA expression of SLC7A5 in TCGA LUAD vs adjacent tissues. (C) Protein expression of SLC7A5 in CTPAC LUAD vs normal tissues. (D) Protein expression of SLC7A5 in CTPAC LUAD vs adjacent tissues. (E) mRNA expression of SLC7A5 in 8 paired LUAD and adjacent tissues from Shandong Province Hospital. (F) mRNA expression of SLC7A5 in 4 LUAD cell lines by qRT-PCR. (G) Protein expression of SLC7A5 in 4 LUAD cell lines by Western blot. The data were presented as the mean ± SD; n = 3. The non-adjusted images were presented in supplementary WB bands 1. (H) mRNA expression of SLC7A5 in TCGA tumors vs normal tissues (if available) by TIMER2. (I) The distribution of SLC7A5 in HCC827 and A549 cells with or without SLC7A5 siRNAs transfection by immunofluorescence. *$P < 0.05$, **$P < 0.01$, ***$P < 0.001$, ****$P < 0.0001$.

collected and 8.47% samples possessed the CNV, of which single deletion was detected in 36 samples and single gain was detected in 11 samples. SLC7A5 expression significantly decreased in samples with single deletion compared to normal samples ($P = 4.3e-05$). The samples with single gain had higher SLC7A5 expression than normal samples ($P = 0.95$) (Figure 3A). For DNA methylation, 9 methylation sites were identified, which were cg01829163, cg03408354, cg27555036, cg00858400, cg12408911, cg08710629, cg00728300, cg26695445, cg07067659 in order of decreasing methylation level (Figure 3B). The overall methylation level was negatively correlated to SLC7A5 expression ($R = -0.36$, $P = 8.2e-16$) (Figure 3C). The correlation of SLC7A5 expression and each methylation site was showed in the radar chart (Figure 3D). To further screen out those prognostic methylation sites affecting SLC7A5 expression, we identified 4 methylation sites according to the following criteria: (1) the correlation coefficient of SLC7A5 expression and methylation level < -0.1, $P < 0.05$; the methylation level was positively related to OS and PFS ($P < 0.05$). They were cg00728300 ($R = -0.4$, $P < 2.2e-16$), cg00858400 ($R = -0.26$, $P = 7.5e-09$), cg12408911 ($R = -0.12$, $P = 0.0073$), cg08710629 ($R = -0.37$, $P = 2.4e-16$). The OS and PFS of the 4 methylation sites were displayed in supplementary figure 3A-3H. To seek

the potential TFs for SLC7A5, we utilized the PROMO website to predict the TFs of SLC7A5. Altogether 16 TFs were obtained when the false tolerance was equal to zero, including CEBPB, GATA1, YY1, TFAP2A, PAX5, SRY, ELK1, STAT4, MYC, SP1, GCF, TFII-1, FOXP3, RXRA, RB1, PRA. Intersecting the upregulated genes in LUAD, the common TFs were TFAP2A and FOXP3. The possible binding sequence for TFAP2A and FOXP3 in the promotor region of SLC7A5 were GCAGGC/GCCTGC, GTTGTG, respectively (Figure 3E). CeRNA plays an important role in the post-transcriptional regulation of gene expression. Based on starBase database, we predicted the miRNAs of SLC7A5 and matched lncRNAs (Figure 3F). Combing the differential expression, prognosis and correlation to SLC7A5, three significantly differential miRNAs were found (miR-30a-5p: $R = -0.35$, $P = 8.8e-16$, Log$_2$fold change $= -1.29$, $P = 6.44e-10$; miR-184: $R = -0.25$, $P = 5.63e-09$, Log$_2$fold change $= -3.37$, $P = 8.11e-18$; miR-195-5p: $R = -0.23$, $P = 1.48e-07$, Log$_2$fold change $= -1.09$, $P = 2.49e-11$) (Figure 3G, H). The high expression of the 3 miRNAs all indicated better prognoses of LUAD patients (Figure 3H). 42 lncRNAs targeted the 3 miRNAs were identified, which were positively related to SLC7A5 expression but negatively related to their miRNAs (Supplementary table 3).
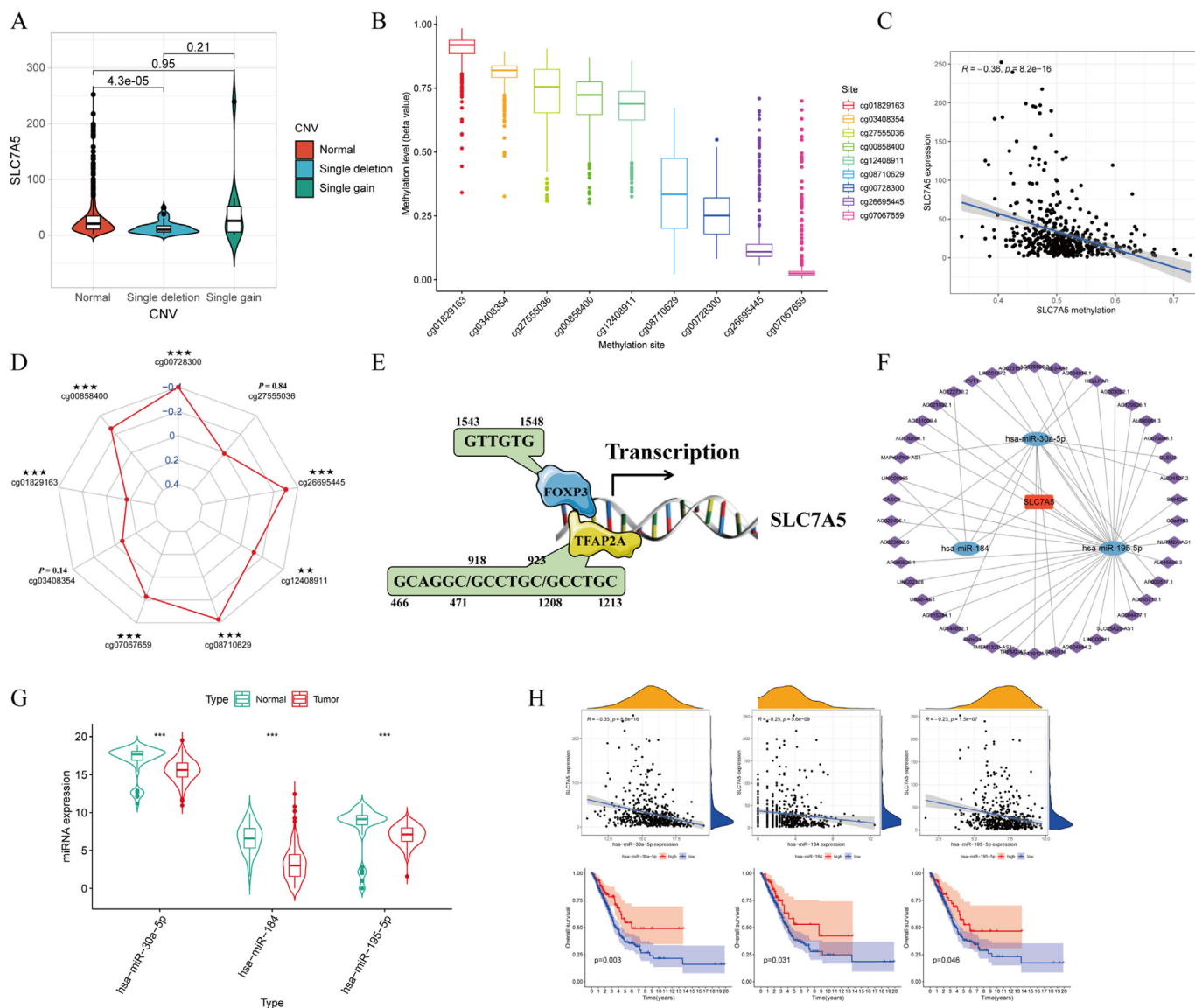
Figure 3. Analysis of copy number variation (CNV), DNA methylation, transcription factors and ceRNA network of SLC7A5. (A) The correlation of CNV and SLC7A5 expression. (B) Methylation levels of various methylation sites of SLC7A5. (C) The correlation of methylation level and SLC7A5 expression. (D) The radar chart represented the correlation of methylation level of each site and SLC7A5 expression. (E) The predicted transcription factors and binding sequence of SLC7A5 by Promo. (F) ceRNA network of SLC7A5 by Cytoscape. (G) expression of 3 predicted miRNAs targeting SLC7A5 in TCGA LAUD vs normal tissues. (H) Upper panel: the correlation of 3 predicted miRNA and SLC7A5 (Spearman Correlation test); bottom panel: Kaplan-Meier survival analysis of corresponding miRNA high- and low-expression groups. The correlation was tested by Spearman Correlation test and the Kaplan-Meier survival analysis was tested by log-rank test. In all the above statistical tests, $P < 0.05$ was considered significant, $*P < 0.05$, $**P < 0.01$, $***P < 0.001$.

3.4. Assessment of prognosis and its clinical relevance

In order to assess the prognostic role of SLC7A5 in LUAD, the OS and PFS analyses were conducted. The survival curves suggested that SLC7A5 high-expression group had worse prognosis than low-expression group whether in OS ($P < 0.001$) or PFS ($P = 0.011$) (Figures 4A, 4B). The Kaplan-Meier plotter showed the consistent conclusion (OS: *HR* 1.83 95%CI 1.45–2.32, $P = 3.5e-07$; PFS: *HR* 1.75 95%CI 1.27–2.4, $P = 4.5e-04$) (Supplementary Figure 4A, 4B). Multiple GEO datasets and 51 LUAD cases from Shandong Province Hospital were used for external validation. The OS of 719 LUAD patients from GEO and 51 LAUD patients from Shandong province hospital all validated that SLC7A5 high-expression group had worse prognosis than low-expression group ($P < 0.05$) (Figure 4C, Supplementary Figure 4C). By univariate and multivariate Cox regression analysis, SLC7A5 expression, age and pathological stage were independent prognostic factors (SLC7A5/20: *HR* 1.162, 95%CI

1.084–1.247, $P < 0.001$; age: *HR* 1.597 95%CI 1.169–2.181, $P = 0.003$; stage: *HR* 1.597 95%CI 1.388–1.838, $P < 0.001$) (Figures 4D, 4E). To investigate its clinical relevance, we analyzed SLC7A5 expression between different clinical subtypes. The results showed that advanced LUAD patients had higher SCL7A5 expression than early-stage patients (Figure 4F). In the other clinical features (age, gender, race, treatment type), there was no significant association ($P < 0.05$) (Supplementary Figure 4D-4H).

3.5. Functional enrichment analysis

To explore the underlying molecular mechanism leading to difference of prognosis between SLC7A5 high- and low-expression groups, we performed the functional enrichment analysis. The results of GO enrichment analysis were significantly related to cell cycle and division, L-amino acid transport, DNA damage repair, apoptosis and cellular
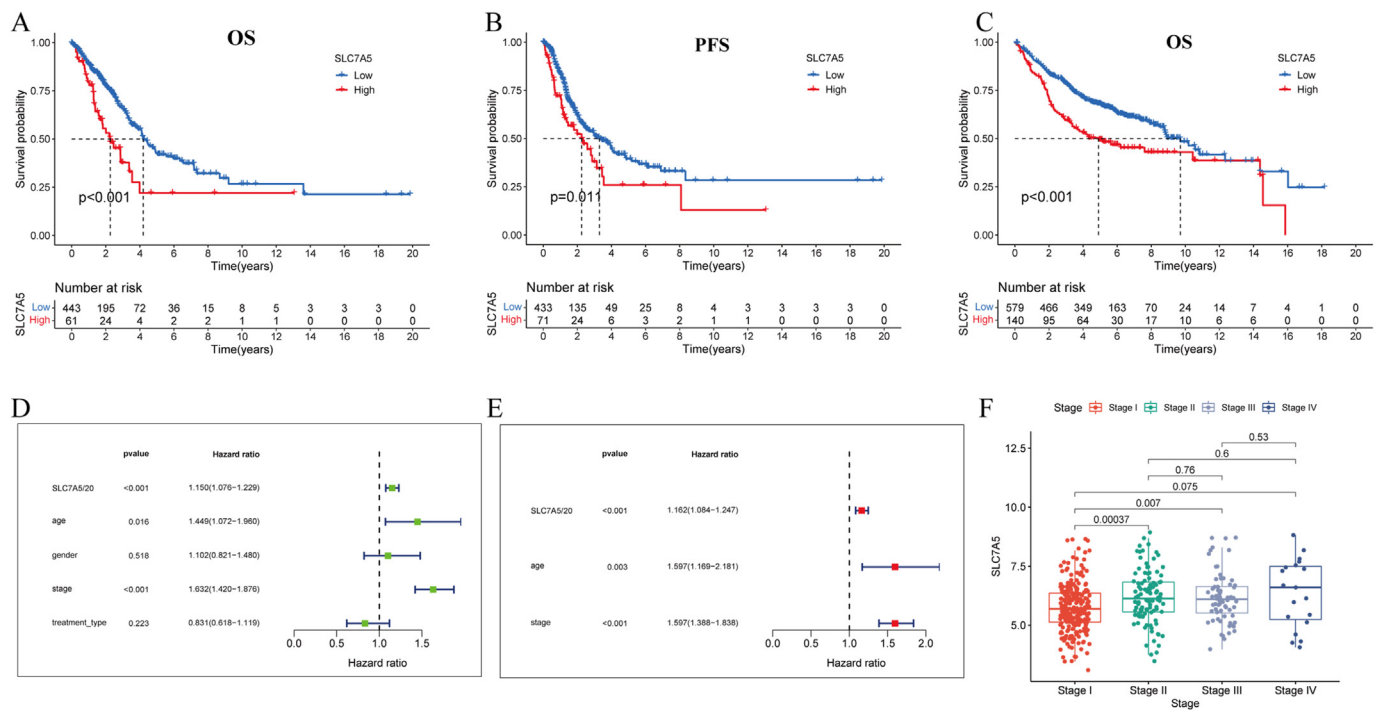
Figure 4. The role of SLC7A5 on LUAD prognosis and its clinical correlation. (A) The overall survival (OS) (A) and progression-free survival (PFS) (B) difference between SLC7A5 high- and low-expression groups in TCGA (OS: $P < 0.001$; PFS: $P = 0.011$). (C) The OS difference between SLC7A5 high- and low-expression groups in the integrated GEO dataset ($P < 0.001$). Univariate (D) and multivariate (E) Cox regression analysis of SLC7A5 expression and clinical features. SLC7A5/20 represented that SLC7A5 expression was divided by 20. (F) The relationship between SLC7A5 expression and pathological stage in LUAD.

response to reactive oxygen species whether in BP, CC or MF (Supplementary Figure 5A-5C). The results of KEGG showed that multiple pathways related to cell cycle and DNA damage repair were enriched in SLC7A5 high-expression group including cell cycle, DNA replication, base excision repair and mismatch repair. Moreover, known as an important tumor-related pathway, Notch signaling pathway was also enriched. In addition, aminoacyl tRNA biosynthesis, citrate cycle TCA cycle and spliceosome were tightly associated with SLC7A5 expression (Supplementary Figure 5D). By GSVA analysis, many pathways and functions were overlapped with GO and KEGG enrichment analysis and a plethora of immune-related function and oncogenic pathways were also annotated (Supplementary Figure 5E). IFN signaling pathway, IL-2/STAT5 signaling, IL-6/JAK/STAT3 signaling, inflammatory response and allograft rejection were more active in SLC7A5 low-expression group. mTORC1 signaling, glycolysis and MYC targets were more concentrated on SLC7A5 high-expression group.

3.6. Landscape of tumor microenvironment

Using "estimate" package, we quantified the stromal, immune and tumor components of LUAD samples. The results suggested that SLC7A5 low-expression had higher stromal and immune scores and lower tumor purity (all P values <0.001) (Figures 5A, 5B). On the aspect of HLA-related molecules and immune checkpoints. SLC7A5 low-expression group had dominant expression of HLA-related genes and 22 immune checkpoints (47.8%) were negatively related to SLC7A5 expression and only 8 immune checkpoints (17.4%) were positively related to SLC7A5 expression (Figures 5C, 5D). It worth mentioning that PD-L1 and CTLA4 both were obviously high expressed in SLC7A5 low-expression group (PD-L1: $P = 0.0019$; CTLA4: $P = 0.011$) (Figures 5E, 5F). The result of TIDE suggested that SLC7A5 low-expression group had significantly higher T cell dysfunction scores and lower T cell exclusion scores than SLC7A5 high-expression group ($P < 0.001$) (Figures 5G, 5H). To explore the immune cells infiltration between the two groups, we use multiple platforms to evaluate the immune cells infiltration such as XCELL, TIMER,

QUANTISEQ, MCPCOUNTER, EPIC, CIBERSORT-ABS, CIBERSORT (Figure 5I). The results showed that most immune cells had negative association with SLC7A5 expression including myeloid dendritic cell, macrophage, mast cell, CD8+ T cell, B cell et al. Considering the bulk data represented the comprehensive expression of SLC7A5 in various cells including tumor cells, immune cells and stromal cells, we investigated SLC7A5 expression in immune cells by the single-cell sequencing data [25]. In NSCLC, SLC7A5 was commonly low expression in tumor-infiltrating CD4+ and CD8+ T cell. CCR7 and LEF1 as the markers of naïve T cell according to the study of Zhang et al [25], we found naïve T cells had lower SLC7A5 expression than the differentiated T cells. Moreover, effect T cell (CD4-GNLY and CD8-CX3CR1) also had lower SLC7A5 expression than the other differentiated immune cell. Although the clusters of CD4-CTLA4, CD4-CXCL13, CD4-GZMA, CD8-ZNF683, CD8-LAYN and CD8-GZMK had higher SLC7A5 expression, they were Treg cell, intermediate functional states T cell and exhausted T cell (Figures 5J, 5K).

3.7. Analysis of immunotherapy efficacy and the sensitivity of chemotherapy drugs

Considering the tight association of SLC7A5 and immunity, we explored the relationship of SLC7A5 expression and immunotherapy efficacy. IPS is developed to predict the response to anti-CTLA-4 and anti-PD-1 regimens. The results suggested that whether a single regimen or combination of anti-CTLA4 and anti-PD-1 regimens, patients from SLC7A5 low-expression group had higher response rate than patients from SLC7A5 high-expression group (all $P < 0.001$) (Figures 6A-6D). In addition, SLC7A5 expression could greatly distinguish the prognoses of patients receiving anti-CTLA4 regimen (Figure 6E). SLC7A5 low-expression group had significant higher survival rate and response rate than SLC7A5 high-expression group (Log-rank test: $P < 0.001$; response rate: low-expression vs high-expression 19% vs 0%) (Figure 6F). Due to high enrichment of mTORC1 signaling, cell cycle and growth factor signaling pathways in SLC7A5 high-expression group, we explored the sensitivity of drugs targeting the pathways. The results showed that
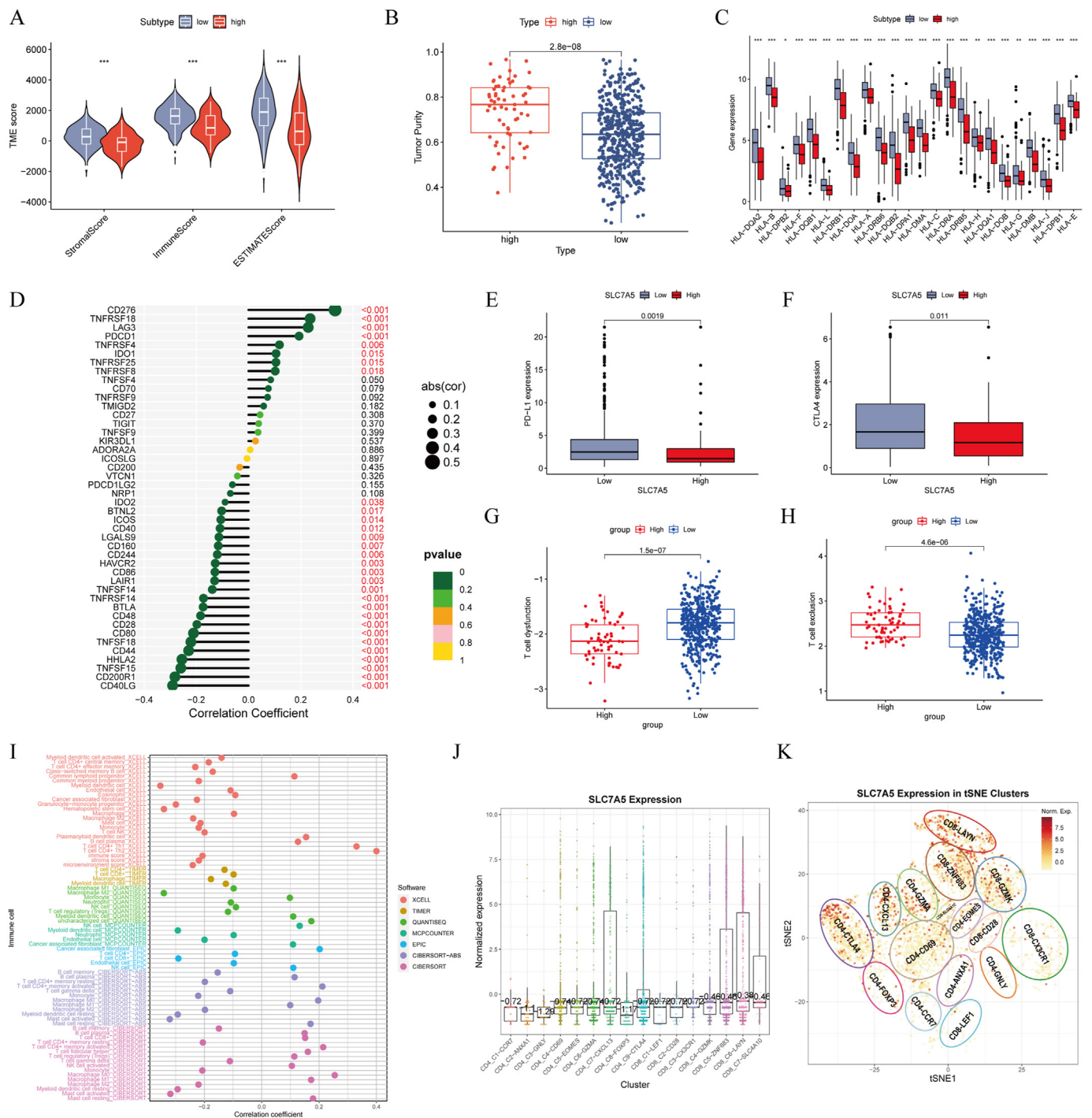
Figure 5. Landscape of tumor microenvironment (TME) between SLC7A5 high- and low-expression groups. (A) The differences of immune scores, stromal scores and estimate scores between SLC7A5 high- and low-expression groups. (B) The correlation of SLC7A5 expression and tumor purity. (C) The differences of HLA-related genes between SLC7A5 high- and low-expression groups. (D) the correlation of SLC7A5 and immune checkpoint genes. The differences of PD-L1 (E) and CTLA4 (F) expression between SLC7A5 high- and low-expression groups. The differences of T cell dysfunction (G) and exclusion (H) between SLC7A5 high- and low-expression groups. (I) the correlation of SLC7A5 expression and tumor-infiltrating immune cells via XCELL, TIMER, QUANTISEQ, MCPCOUNTER, EPIC, CIBERSORT-ABS, CIBERSORT. (J) SLC7A5 expression in various T cells subtypes in non-small cell lung cancer by single-cell sequencing data. (K) SLC7A5 expression in 16 main T cell subtypes projected by t-SNE based on single-cell sequencing data. *$P < 0.05$, **$P < 0.01$, ***$P < 0.001$, ****$P < 0.0001$.

SCL7A5 high-expression group were more sensitive to the drugs (inhibitors of mTORC1 pathway: CMK $P = 0.00074$, PF.4708671 $P = 4.3$e-08; inhibitors of cell cycle: Cytarabine $P = 0.039$, Docetaxel $P = 4.4$e-08, Paclitaxel $P = 0.0013$, RO.3306 $P = 1.2$e-11, Roscovitine $P = 0.00021$, Vinblastine $P = 0.00091$; growth factor signaling pathways: OSI.906 (inhibitors of IGF-1R) $P = 2.4$e-05, Axitinib (inhibitor of VEGFR) $P = 0.0051$) (Figure 6G-6P).

3.8. The correlation of SLC7A5 expression and other malignant indicators by ssGSEA

By ssGSEA, we quantified multiple malignant indicators including AA score, EMT, DNA damage response, hypoxia and cancer stemness. LUAD had significantly higher AA score than the normal tissues ($P = 7.2$e-04) (Figure 7A) and SLC7A5 expression was positively related to AA score
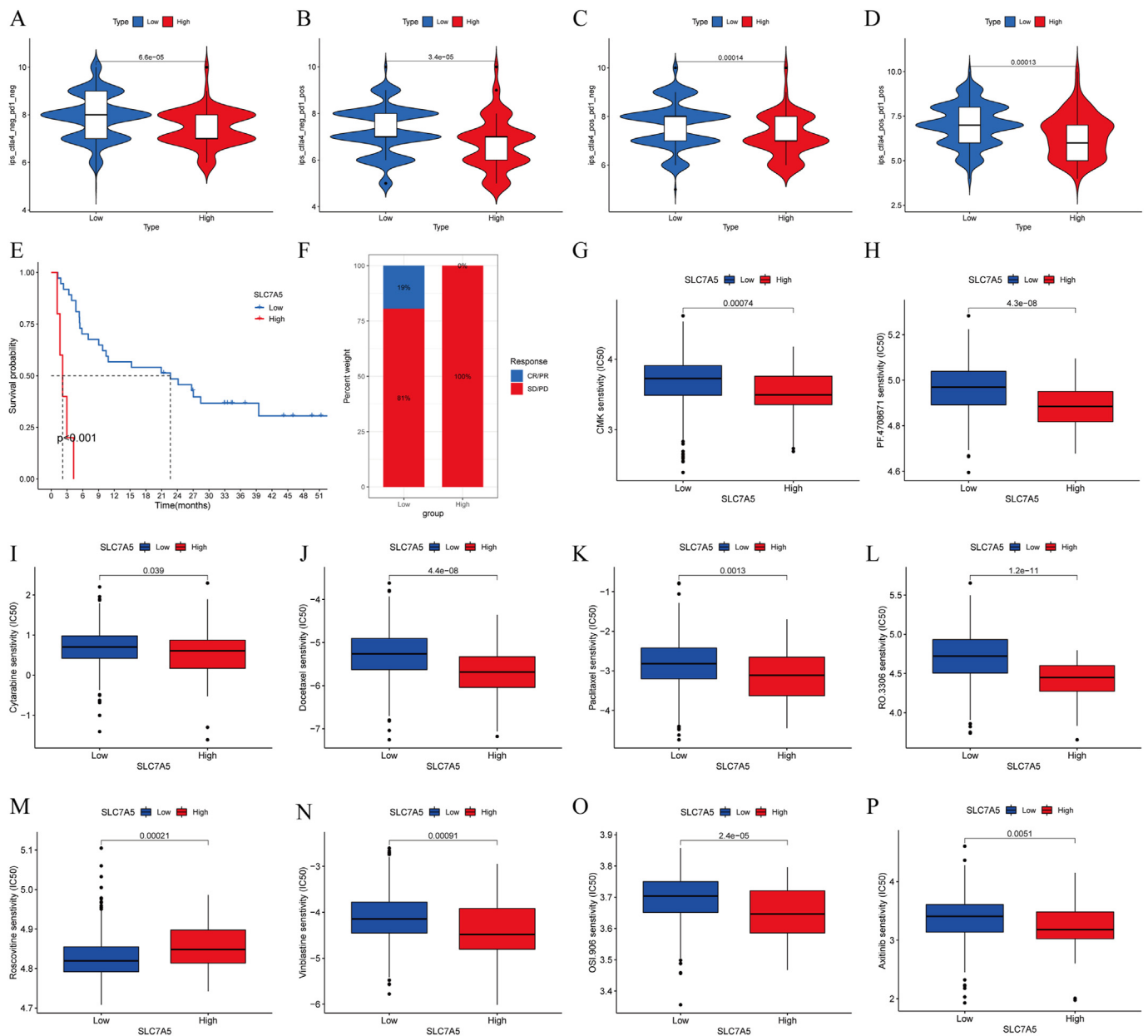
Figure 6. Analysis of immunotherapy efficacy and the sensitivity of chemotherapy drugs. The difference of immunotherapy efficacy between SLC7A5 high- and low-expression groups. (A) Without anti-PD-1 and anti-CTLA4 regimens; (B) Anti-PD-1 regimen; (C) Anti-CTLA4 regimen; (D) Combination of anti-PD-1 and anti-CTLA4 regimens. (E) the Kaplan-Meier survival analysis of SLC7A5 high- and low-expression groups in an independent immunotherapy cohort receiving anti-CTLA4 regimen. (F) the difference of response rates between SLC7A5 high- and low-expression groups with anti-CTLA4 regimen. CR: complete response; PR: partial response; SD: stable disease; PD: progressive disease. (CR/PR: SLC7A5 high-expression group vs SLC7A5 low-expression group: 19% vs 0%). The chemotherapy sensitivity between SLC7A5 high- and low-expression groups. Inhibitors of mTORC1 pathway: (G) CMK, (H) PF.4708671; inhibitors of cell cycle: (I) Cytarabine, (J) Docetaxel, (K) Paclitaxel, (L) RO.3306, (M) Roscovitine, (N) Vinblastine; growth factor signaling pathways: (O) OSI.906 (inhibitors of IGF-1R), (P) Axitinib (inhibitor of VEGFR).

in LUAD ($R = 038$, $P < 2.2e{-}16$) (Figure 7B). Moreover, high SLC7A5 expression had strong correlation with EMT, DNA damage response, hypoxia, and cancer stemness (EMT: $R = 0.53$, $P < 2.2e{-}16$; DNA damage response: $R = 0.43$, $P < 2.2e{-}16$; hypoxia: $R = 0.24$, $P = 1.8e{-}08$; DNAss: $R = 0.19$, $P = 8.6e{-}05$; RNAss: $R = 0.37$, $P = 9.1e{-}16$) (Figures 7C-7G). The correlation of SLC7A5 and the other AATs expression suggested that SLC7A5 had an obviously positive correlation with SLC3A2, SLC1A5 and SLC7A1 ($R = 0.68$, 0.36, 0.46, respectively) (Supplementary Figure 6). There was no significant association with the other AATs. TMB was an important signature to predict immunotherapy efficacy but it had no statistical correlation with SLC7A5 expression ($R = 0.064$, $P = 0.15$) (Figure 7H). There were 96.67% patients with gene alteration in SLC7A5

high-expression group and 87.56% patients with gene alteration in SLC7A5 low-expression group (Figures 7I, 7J).

3.9. SLC7A5 deficiency in LUAD cells suppresses proliferation, migration, mTORC1 pathway activity and is less sensitive to rapamycin in vitro

To validate the role of SLC7A5 in LUAD, we knocked down SLC7A5 expression by siRNA in two LUAD cell lines (A549, PC9) and then did proliferation and wound healing assays. The proliferation assay reflected that SLC7A5 deficiency could obviously suppress proliferation of LUAD cells (Figures 8A, 8B). In wound healing assay, the ability to migrate was greatly attenuated in LUAD cells when SLC7A5 expression
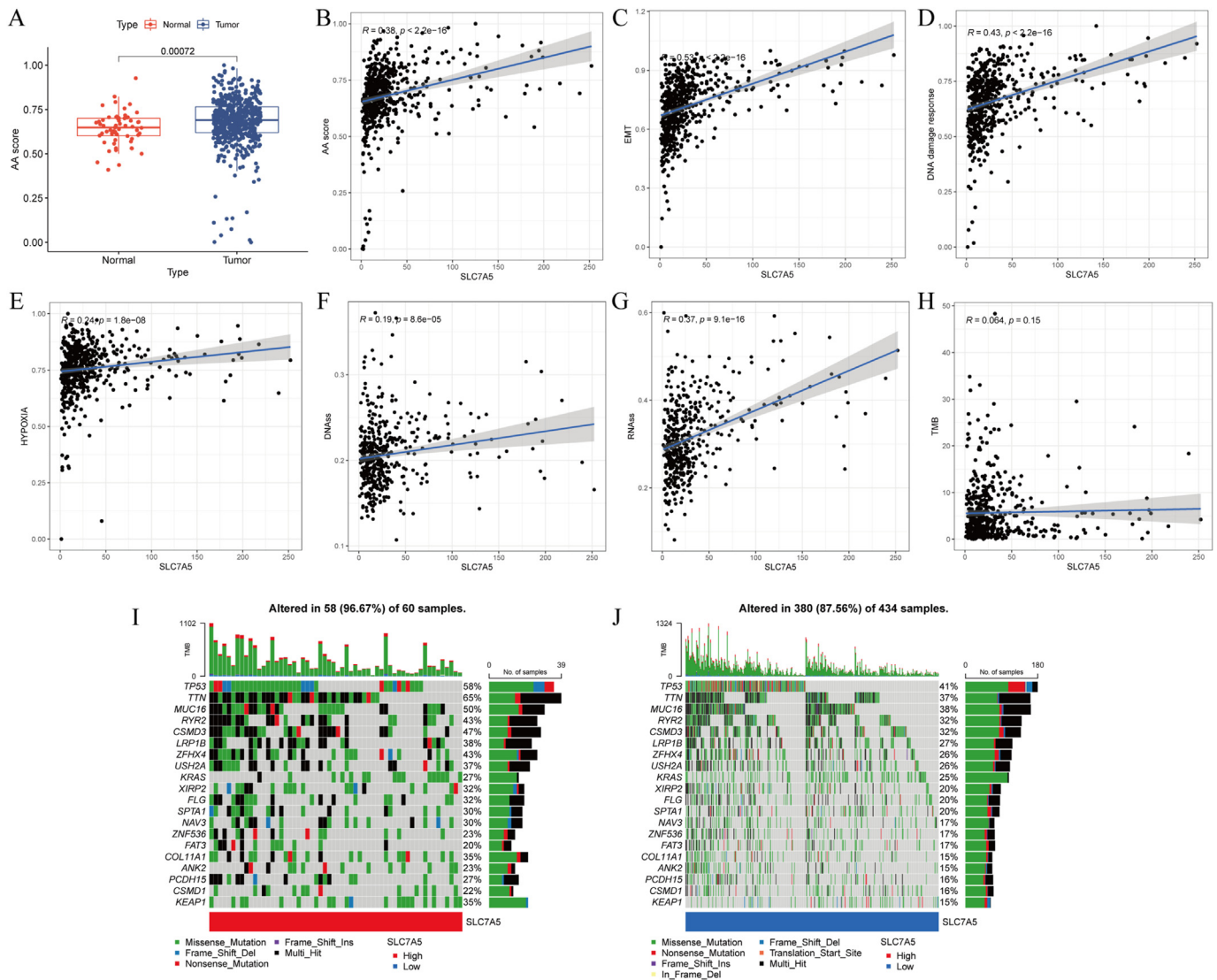
Figure 7. The correlation of SLC7A5 expression and other malignant indicators by ssGSEA. (A) Amino acid score (AA score) between normal tissue and LUAD. (B) Correlation of SLC7A5 and AA score. (C) Correlation of SLC7A5 and EMT score. (D) Correlation of SLC7A5 and DNA damage response score. (E) Correlation of SLC7A5 and hypoxia score. Correlation of SLC7A5 and cancer stemness: (F) DNAss, (G) RNAss. (H) Correlation of SLC7A5 and tumor mutation burden (TMB). (I) The landscape of gene mutation in SLC7A5 high-expression group. (J) The landscape of gene mutation in SLC7A5 low-expression group.

was interfered by siRNA (Figures 8C, 8D). SLC7A5 deficiency in LUAD cells decreased the sensitivity to rapamycin (IC50 (95%CI) μM: A549 Ctrl 8.35 (6.36–11.09), siRNA#1 28.29 (18.17–44.28), siRNA#2 23.61 (14.88–38.03); PC9 Ctrl 16.17 (12.48–21.08), siRNA#1 42.03 (34.48–51.33), siRNA#2 58.38 (49.44–69.10)) (Figures 8E, 8F). The main indictors of epithelial-mesenchymal transition (EMT) including TWIST1, SNAIL1/2, CDH1 had significantly decreasing expression in SLC7A5 knockdown cells (Figure 8G). In addition, we also investigated the differential expression of indicators of DNA damage response and hypoxia between control and SLC7A5 knockdown cells. TP53, XRCC5, XRCC6, RAD51, ATM, BRCA1, BRACA2 and PRKDC were down-regulated in SLC7A5 knockdown cells (Figure 8H). Hypoxia, angio-genesis and growth factor related genes (HIF-1α, EGFR, VEGF-α, PDGFR-α) in SLC7A5 knockdown cells had decreasing expression (Figure 8I). In addition, the protein expression levels of p-AKT (Ser473), p-mTOR (Ser2448) were significantly decreased but the total proteins expression was not changed when SLC7A5 expression was knocked down (Figures 8J, 8K). It was suggested that the activity of mTORC1 pathway was suppressed in LUAD cells with SLC7A5 low expression.

4. Discussion

Lung cancer is still the main cause of cancer-related death and LUAD is the most common histological subtype, accounting for 40% [1]. Though the great progress in the treatment including targeted therapy and immunotherapy, the 5-year OS rate of LUAD is less than 20% [28, 29]. The heterogeneity of tumor and immunosuppressive TME are main factors leading to treatment failure, metastasis and relapse [30, 31]. Due to the interaction of amino acid metabolism and TME, increasing studies pay attention to amino acid metabolism of immune cells and tumor cells and AATs begin to acquire more concentration. Here, we identified LUAD-specific prognostic AATs SLC7A5 and depicted its differential expression profiles and intracellular distribution. High SLC7A5 expression indicated poor prognosis and advanced pathological stage. Cell cycle, DNA damage repair, response to reactive oxygen and mTORC1 signaling pathway were hyperactive in SLC7A5 high-expression group. However, SLC7A5 high-expression group had less expression of HLA-related genes and immune checkpoints and less immune cell infil-tration. More importantly, tumor-infiltrating immune cells had commonly low expression of SLC7A5 and effect T cell (CD4-GNLY and
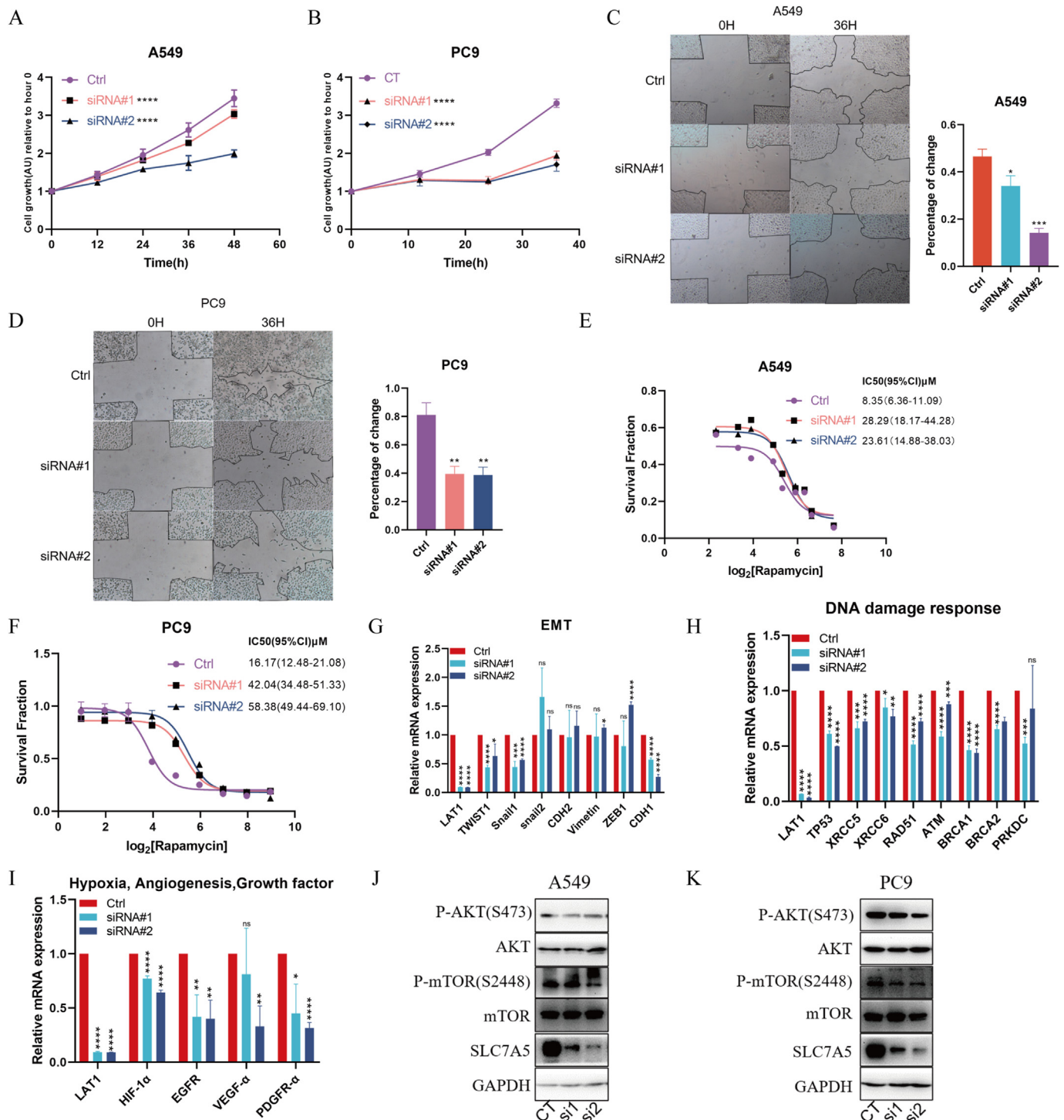
Figure 8. SLC7A5 deficiency in LUAD cells suppresses tumor proliferation, migration, mTORC1 pathway activity and is less sensitive to rapamycin in vitro. A549 cells (A) and PC9 cells (B) transfected by SLC7A5 siRNAs were used for cell proliferation assay. A549 cells (C) and PC9 cells (D) transfected by SLC7A5 siRNAs were used for wound healing assay. The data were presented as the mean ± SD; n = 3. The cell viability of A549 cells (E) and PC9 cells (F) transfected by SLC7A5 siRNAs was assessed by SRB dyeing assays with rapamycin treatment. The data were presented as the mean ± SD; n = 6. Indicators of Epithelial-mesenchylmal transition (EMT) (G), DNA damage response (H), hypoxia, angiogenesis, and growth factors signaling (I) were detected by qRT-PCR in PC9 cells transfected by SLC7A5 siRNAs. The indicated proteins related to mTORC1 pathway were detected by western blotting in A549 (J) and PC9 (K) cells with or without SLC7A5 siRNAs. The non-adjusted images were presented in supplementary WB bands 2 and 3, respectively. *P < 0.05, **P < 0.01, ***P < 0.001, ****P < 0.0001.

CD8-CX3CR1) also had lower SLC7A5 expression than the other differentiated immune cell. Chemotherapy drugs targeted mTORC1 pathway, cell cycle and angiogenesis had more sensitivity in SLC7A5 high-expression group based on bioinformatic analyses. The results of western blotting and cell viability assays also validated the change of

mTORC1 pathway activity and sensitivity to rapamycin when SLC7A5 expression was knocked down in LUAD cells, which was consistent with the results of bioinformatic analyses.

SLC7A5, also known as LAT1, forms a heteromeric L-type AAT complex with SLC3A2, which stabilizes SLC7A5 and facilitates its

translocation to the plasma membrane [32]. SLC7A5 mediates large neutral amino acids transportation across plasma membrane in a Na+ independent manner, which supplies essential amino acid for somatic cells [33, 34]. SLC7A5 is not only involved in suppling amino acids to cancer cells but also oncogenic signaling pathways such as mTORC1 signaling pathway [35]. Herein, we found SLC7A5 was significantly high expression in LUAD whether in transcription or translation level. Most of 33 tumors had aberrant expression of SLC7A5 from TCGA database. The phenomenon was also validated in many literatures, which implied tumor cells may occupy more nutrients via upregulation of SLC7A5 expression. Based on its cancer-specific expression, clinical PET studies using SLC7A5-specific probe FAMT have been conducted in patients with malignant tumors and FAMT is specifically accumulated in malignant tumors with low physiologic background [36, 37]. As a result, SLC7A5 is promising to be popularized in clinical as a non-invasive diagnostic technique for cancer.

We found that SLC7A5 had an obviously positive correlation with SLC3A2, SLC1A5 and SLC7A1. It has been reported that SLC1A5, SLC7A5 and SLC3A2 coordinately exert a vital role on activation of mTORC1 pathway. Cellular uptake of L-glutamine is the rate limiting step for essential amino acids (EAA)- and growth factor-regulation of mTORC1. SLC1A5 is a high affinity L-glutamine transporter and responsible for uptake of L-glutamine. SLC7A5/SLC3A2 is a hetero-dimeric bidirectional antiporter that regulates the exchange of intra-cellular L-glutamine for extracellular L-leucine. Then the intracellular EAA will activate mTORC1 signaling [38]. So the co-expression of SLC1A5, SLC7A5 and SLC3A2 may be beneficial to regulation of signaling pathways. SLC7A1 belongs to the cationic amino acid transporters (CATs) and SLC7A5 belongs to the L-type amino acid transporters (LATs). Members of the CAT family transport predominantly cationic amino acids by facilitating diffusion with intracellular substrates [39]. At present, the redundant function between SLC7A5 and SLC7A1 is reported minimally. So, SLC7A5 seems to exert an indispensable function in cells.

Multiple datasets verified that LUAD patients with high SLC7A5 expression had poor OS and PFS. With the progression of LUAD, SLC7A5 expression was increased. Univariate and multivariate Cox regression suggested that SLC7A5 was an independent prognostic factor of LUAD. Previous literatures have reported that SLC7A5 expression was associated with poor prognosis of multiple tumors. Li et al. reported that SLC7A5 served as a prognostic factor of breast cancer and promoted cell proliferation [35, 36]. Ding et al. found that GSE1 predicted poor survival outcome in gastric cancer by SLC7A5 enhancement of tumor growth and metastasis [40]. However, the molecular mechanism of SLC7A5 over-expression causing poor prognosis has not been clarified completely. Up to now, SLC7A5 is more regarded as the upstream of mTORC1 signaling pathway. To explore the other mechanism of SLC7A5 on prognosis, functional enrichment analysis was performed and revealed that SLC7A5 expression was tightly associated with mTORC1 pathway, cell cycle, and angiogenesis. The chemotherapy drug sensitivity analyses indirectly demonstrated that these pathways were hyperactive in SLC7A5 high-expression group. The results of qRT-PCR suggested that SLC7A5 deficiency would decrease key genes of EMT, DNA damage response and various growth factors signaling. Summarizing the above results, we can come to the following conclusions. Firstly, SLC7A5 is AAT to increase intracellular essential amino acids concentration, thus supplying nutrients for proliferation and activating mTORC1 signaling pathway in tumor cells. Secondly, SLC7A5 may promote proliferation and chemotherapy resistance by various growth factors signaling pathway and DNA damage response. Thirdly, SLC7A5 may mediate invasion and metastasis by promoting EMT and angiogenesis.

However, TME is an indivisible whole and the interaction of tumor cells and immune cells cannot be neglected in the development and treatment of tumor. Interestingly, we found higher expression of HLA-related genes, immune checkpoint genes and immune infiltrating cells in SLC7A5 low-expression group. the single-cell sequencing data reflected that SLC7A5 was commonly low expression in various immune cells and naïve T cells had lower SLC7A5 expression than the differentiated T cells. Moreover, effect T cell had lower SLC7A5 expression than Treg cell, intermediate functional states T cell and exhausted T cell. The weak expression of SLC7A5 in immune cells made them at a disadvantage when competing with tumor cells for nutrients. Furthermore, among immune cells, the effector T cell had weaker ability to acquire amino acids than Treg cell et al. c-Myc is essential for NK cell metabolism and activity upon IL-2/IL-12 stimulation as well as for CD3/CD28 mediated metabolic reprogramming and activation of T cells [41, 42]. AATs including SLC1A5, SLC7A5 and SLC3A2 upregulates c-Myc, which then stimulates the expression of these AATs. In this positive feedback loop, the proliferation and activation of T cell and NK cell are further enhanced [16]. Additionally, when pro-inflammatory cytokines activate the effector functions of lymphocytes, it tends to induce the upregulation of proteins involved in AATs, such as SLC7A5, SLC3A2 and SLC1A5. For example, IL-2 stimulation of CD8 T cells will increase SLC7A5 expression in a time-dependent manner [43, 44]. In NK cells, IL-2 can upregulate SLC1A5 and SLC7A5/SLC3A2, and these transporters are needed for IFN-γ production and degranulation [45]. Since a robust metabolism in immune cells is required for differentiation and optimal anti-tumor effector functions, the unbalance expression severely impaired anti-tumor immunity [16]. The IPS and immunotherapy cohort (anti-CTLA4) both suggested SLC7A5 low-expression group had higher response rate and longer survival time than SLC7A5 high-expression group. Consequently, upregulating SLC7A5 in TILs and downregulating it in tumor cells may reshape the immunosuppressive TME and enhance anti-tumor immunity.

To reverse the expression of SLC7A5 in LUAD, we identified several aspects affecting transcription and translation of SLC7A5. Enhancing the methylation levels of the four methylation sites including cg00728300, cg00858400, cg12408911 and cg08710629 may significantly decrease SLC7A5 expression. Designing small molecule compounds targeting FOXP3, TFAP2A may obviously inhibit the transcription of SLC7A5. In addition, miRNAs targeting SLC7A5 were shown as miR-30a-5p, miR-184, miR-195-5P, of which the regulation between SLC7A5 and miR-184 has been validated in retinoblastoma [46]. The corresponding lncRNAs also be identified. So, targeting these molecules in immune cells and tumor cells may reverse the unbalanced expression.

5. Conclusions

In summary, as a LUAD-specific prognostic AAT, SLC7A5 is involved in activation of multiple pathways including mTORC1 signaling pathway, cell cycle, various growth factors signaling pathways, EMT, angiogenesis and DNA damage response to promote proliferation, migration, metastasis and chemotherapy resistance, thus indicating poor prognosis. Moreover, SLC7A5 may participate in forming immunosuppressive TME and associated with low response of immunotherapy. SLC7A5 is promising to be a new diagnostic and prognostic biomarker and therapeutic target in LUAD.

Declarations

Author contribution statement

Yong Liu: Conceived and designed the experiments; Performed the experiments; Analyzed and interpreted the data; Wrote the paper.

Guoyuan Ma: Conceived and designed the experiments.

Jichang Liu; Haotian Zheng; Gemu Huang; Qingtao Song: Contributed reagents, materials, analysis tools or data.

Zhaofei Pang: Conceived and designed the experiments; Performed the experiments; Analyzed and interpreted the data.

Jiajun Du: Conceived and designed the experiments; Wrote the paper.

Data availability statement

Data included in article/supp. material/referenced in article.

Declaration of interest's statement

The authors declare no conflict of interest.

Additional information

Supplementary content related to this article has been published online at https://doi.org/10.1016/j.heliyon.2022.e10866.

References

[1] R.L. Siegel, K.D. Miller, H.E. Fuchs, A. Jemal, Cancer statistics, 2021, CA Cancer J Clin 71 (1) (2021) 7–33.

[2] B.D. Hutchinson, G.S. Shroff, M.T. Truong, J.P. Ko, Spectrum of lung adenocarcinoma, Semin. Ultrasound CT MR 40 (3) (2019) 255–264.

[3] S.M. Gadgeel, S.S. Ramalingam, G.P. Kalemkerian, Treatment of lung cancer, Radiol Clin North Am 50 (5) (2012) 961–974.

[4] F.R. Hirsch, G.V. Scagliotti, J.L. Mulshine, R. Kwon, W.J. Curran, Y.-L. Wu, et al., Lung cancer: current therapies and new targeted treatments, Lancet 389 (10066) (2017) 299–311.

[5] Y. Yang, Cancer immunotherapy: harnessing the immune system to battle cancer, J. Clin. Invest. 125 (9) (2015) 3335–3337.

[6] Z. Wang, Z. Wu, Y. Liu, W. Han, New development in CAR-T cell therapy, J. Hematol. Oncol. 10 (1) (2017) 53.

[7] P. Jiang, S. Gu, D. Pan, J. Fu, A. Sahu, X. Hu, et al., Signatures of T cell dysfunction and exclusion predict cancer immunotherapy response, Nat. Med. 24 (10) (2018) 1550–1558.

[8] N.R. Anderson, N.G. Minutolo, S. Gill, M. Klichinsky, Macrophage-based approaches for cancer immunotherapy, Cancer Res. 81 (5) (2021) 1201–1208.

[9] C.Y. Slaney, M.H. Kershaw, P.K. Darcy, Trafficking of T cells into tumors, Cancer Res. 74 (24) (2014) 7168–7174.

[10] Y. Zhang, H.C.J. Ertl, Starved and asphyxiated: how can CD8(+) T cells within a tumor microenvironment prevent tumor progression, Front. Immunol. 7 (2016) 32.

[11] E.K. Moon, L.-C. Wang, D.V. Dolfi, C.B. Wilson, R. Ranganathan, J. Sun, et al., Multifactorial T-cell hypofunction that is reversible can limit the efficacy of chimeric antigen receptor-transduced human T cells in solid tumors, Clin. Cancer Res. 20 (16) (2014) 4262–4273.

[12] H. Wang, G. Kaur, A.I. Sankin, F. Chen, F. Guan, X. Zang, Immune checkpoint blockade and CAR-T cell therapy in hematologic malignancies, J. Hematol. Oncol. 12 (1) (2019) 59.

[13] E.J. Wherry, T cell exhaustion, Nat. Immunol. 12 (6) (2011) 492–499.

[14] D.M. O'Rourke, M.P. Nasrallah, A. Desai, J.J. Melenhorst, K. Mansfield, J.J.D. Morrissette, et al., A single dose of peripherally infused EGFRvIII-directed CAR T cells mediates antigen loss and induces adaptive resistance in patients with recurrent glioblastoma, Sci. Transl. Med. 9 (399) (2017).

[15] M. Reina-Campos, J. Moscat, M. Diaz-Meco, Metabolism shapes the tumor microenvironment, Curr. Opin. Cell Biol. 48 (2017) 47–53.

[16] M. Nachef, A.K. Ali, S.M. Almutairi, S.H. Lee, Targeting SLC1A5 and SLC3A2/SLC7A5 as a potential strategy to strengthen anti-tumor immunity in the tumor microenvironment, Front. Immunol. 12 (2021), 624324.

[17] D. O'Sullivan, D.E. Sanin, E.J. Pearce, E.L. Pearce, Metabolic interventions in the immune response to cancer, Nat. Rev. Immunol. 19 (5) (2019) 324–335.

[18] M. Song, T.A. Sandoval, C.-S. Chae, S. Chopra, C. Tan, M.R. Rutkowski, et al., IRE1α-XBP1 controls T cell function in ovarian cancer by regulating mitochondrial activity, Nature 562 (7727) (2018) 423–428.

[19] D. Klysz, X. Tai, P.A. Robert, M. Craveiro, G. Cretenet, L. Oburoglu, et al., Glutamine-dependent α-ketoglutarate production regulates the balance between T helper 1 cell and regulatory T cell generation, Sci. Signal. 8 (396) (2015) ra97.

[20] L. Araujo, P. Khim, H. Mkhikian, C.-L. Mortales, M. Demetriou, Glycolysis and glutaminolysis cooperatively control T cell function by limiting metabolite supply to N-glycosylation, Elife 6 (2017).

[21] M.J. Goldman, B. Craft, M. Hastie, K. Repečka, F. McDade, A. Kamath, et al., Visualizing and interpreting cancer genomics data via the Xena platform, Nat. Biotechnol. 38 (6) (2020) 675–678.

[22] E.M. Van Allen, D. Miao, B. Schilling, S.A. Shukla, C. Blank, L. Zimmer, et al., Genomic correlates of response to CTLA-4 blockade in metastatic melanoma, Science 350 (6257) (2015) 207–211.

[23] P. Kandasamy, G. Gyimesi, Y. Kanai, M.A. Hediger, Amino acid transporters revisited: new views in health and disease, Trends Biochem. Sci. 43 (10) (2018) 752–789.

[24] J.-H. Li, S. Liu, H. Zhou, L.-H. Qu, J.-H. Yang, starBase v2.0: decoding miRNA-ceRNA, miRNA-ncRNA and protein-RNA interaction networks from large-scale CLIP-Seq data, Nucleic Acids Res. 42 (Database issue) (2014) D92–D97.

[25] X. Guo, Y. Zhang, L. Zheng, C. Zheng, J. Song, Q. Zhang, et al., Global characterization of T cells in non-small-cell lung cancer by single-cell sequencing, Nat. Med. 24 (7) (2018) 978–985.

[26] P. Charoentong, F. Finotello, M. Angelova, C. Mayer, M. Efremova, D. Rieder, et al., Pan-cancer immunogenomic analyses reveal genotype-immunophenotype relationships and predictors of response to checkpoint blockade, Cell Rep. 18 (1) (2017) 248–262.

[27] P. Geeleher, N. Cox, R.S. Huang, pRRophetic: an R package for prediction of clinical chemotherapeutic response from tumor gene expression levels, PLoS One 9 (9) (2014), e107468.

[28] J. Wu, L. Li, H. Zhang, Y. Zhao, H. Zhang, S. Wu, et al., A risk model developed based on tumor microenvironment predicts overall survival and associates with tumor immunity of patients with lung adenocarcinoma, Oncogene 40 (26) (2021) 4413–4424.

[29] E. Bender, Epidemiology: the dominant malignancy, Nature 513 (7517) (2014) S2–S3.

[30] P.R. Prasetyanti, J.P. Medema, Intra-tumor heterogeneity from a cancer stem cell perspective, Mol. Cancer 16 (1) (2017) 41.

[31] D.F. Quail, J.A. Joyce, Microenvironmental regulation of tumor progression and metastasis, Nat. Med. 19 (11) (2013) 1423–1437.

[32] L.H. Alfarsi, R. El-Ansari, M.L. Craze, B.K. Masisi, O.J. Mohammed, I.O. Ellis, et al., Co-expression effect of SLC7A5/SLC3A2 to predict response to endocrine therapy in oestrogen-receptor-positive breast cancer, Int. J. Mol. Sci. 21 (4) (2020).

[33] M. Galluccio, P. Pingitore, M. Scalise, C. Indiveri, Cloning, large scale over-expression in E. coli and purification of the components of the human LAT 1 (SLC7A5) amino acid transporter, Protein J. 32 (6) (2013) 442–448.

[34] J. Wang, X. Fei, W. Wu, X. Chen, L. Su, Z. Zhu, et al., SLC7A5 functions as a downstream target modulated by CRKL in metastasis process of gastric cancer SGC-7901 cells, PLoS One 11 (11) (2016), e0166147.

[35] Y. Li, W. Wang, X. Wu, S. Ling, Y. Ma, P. Huang, SLC7A5 serves as a prognostic factor of breast cancer and promotes cell proliferation through activating AKT/mTORC1 signaling pathway, Ann. Transl. Med. 9 (10) (2021) 892.

[36] T. Inoue, K. Koyama, N. Oriuchi, S. Alyafei, Z. Yuan, H. Suzuki, et al., Detection of malignant tumors: whole-body PET with fluorine 18 alpha-methyl tyrosine versus FDG–preliminary study, Radiology 220 (1) (2001) 54–62.

[37] K. Kaira, N. Oriuchi, Y. Otani, K. Shimizu, S. Tanaka, H. Imai, et al., Fluorine-18-alpha-methyltyrosine positron emission tomography for diagnosis and staging of lung cancer: a clinicopathologic study, Clin. Cancer Res. 13 (21) (2007) 6369–6378.

[38] P. Nicklin, P. Bergman, B. Zhang, E. Triantafellow, H. Wang, B. Nyfeler, et al., Bidirectional transport of amino acids regulates mTOR and autophagy, Cell 136 (3) (2009) 521–534.

[39] D. Fotiadis, Y. Kanai, M. Palacín, The SLC3 and SLC7 families of amino acid transporters, Mol. Aspect. Med. 34 (2-3) (2013) 139–158.

[40] K. Ding, S. Tan, X. Huang, X. Li, R. Fan, et al., GSE1 predicts poor survival outcome in gastric cancer patients by SLC7A5 enhancement of tumor growth and metastasis, J. Biol. Chem. 293 (11) (2018) 3949–3964.

[41] R.M. Loftus, N. Assmann, N. Kedia-Mehta, K.L. O'Brien, A. Garcia, C. Gillespie, et al., Amino acid-dependent cMyc expression is essential for NK cell metabolic and functional responses in mice, Nat. Commun. 9 (1) (2018) 2341.

[42] R. Wang, C.P. Dillon, L.Z. Shi, S. Milasta, R. Carter, D. Finkelstein, et al., The transcription factor Myc controls metabolic reprogramming upon T lymphocyte activation, Immunity 35 (6) (2011) 871–882.

[43] L.V. Sinclair, J. Rolf, E. Emslie, Y.-B. Shi, P.M. Taylor, D.A. Cantrell, Control of amino-acid transport by antigen receptors coordinates the metabolic reprogramming essential for T cell differentiation, Nat. Immunol. 14 (5) (2013) 500–508.

[44] M. Scalise, M. Galluccio, L. Console, L. Pochini, C. Indiveri, The human SLC7A5 (LAT1): the intriguing histidine/large neutral amino acid transporter and its relevance to human health, Front. Chem. 6 (2018) 243.

[45] H. Jensen, M. Potempa, D. Gotthardt, L.L. Lanier, Cutting edge: IL-2-Induced expression of the amino acid transporters SLC1A5 and CD98 is a prerequisite for NKG2D-mediated activation of human NK cells, J. Immunol. 199 (6) (2017) 1967–1972.

[46] T.-G. He, Z.-Y. Xiao, Y.-Q. Xing, H.-J. Yang, H. Qiu, J.-B. Chen, Tumor suppressor miR-184 enhances Chemosensitivity by directly inhibiting SLC7A5 in retinoblastoma, Front. Oncol. 9 (2019) 1163.